DALTON

Group 9 metal 1,1′-bis(phosphino)ferrocene complexes: synthesis, structures, solution conformation and unusual reactivity

Anthony G. Avent, Robin B. Bedford, Penny A. Chaloner,* Shaliza Z. Dewa and Peter B. Hitchcock

School of Chemistry and Molecular Sciences, University of Sussex, Falmer, Brighton BN1 9QJ, UK

The crystal structure of $[Ir(cod)(L–L)]^+$ **3** [cod = cycloocta-1,5-diene, L–L = 1-(diisopropylphosphino)-1′-(diphenylphosphino)ferrocene] can be related to those of the analogous complexes with L–L = 1,1′-bis(diphenylphosphino)ferrocene (dppf) **1** and 1,1′-bis(diisopropylphosphino)ferrocene (disppf), **2**, all the complexes being readily synthesized from $[Ir(cod)(py)_2]^+$ (py = pyridine). An optimum diphosphine bite angle of approximately 99° is maintained in all three complexes by varying the twist of the ferrocene, which decreases with increasing steric profile of the phosphine, and by distortion of the geometry at the iridium atom away from square planar towards tetrahedral. The twist about the ferrocene moiety induces chirality at the iridium atom in all three complexes and the interchange of stereoisomers can be followed by variable-temperature ^1H NMR spectroscopy. Application of the Eyring equation gave approximate values of $\Delta G^{\ddagger}$ for this process of 36.1 ± 0.2, 39.3 ± 0.2 and 34.3 ± 0.2 kJ mol^{-1} for **1**–**3** respectively. The ligand disoppf also induces considerable distortion away from square-planar geometry in the complex $[Rh(nbd)(disoppf)][BF_4]$ **4** {nbd = norbornadiene (bicyclo[2.2.1]hepta-2,5-diene)}, as found in a crystal structure determination, which may account for the unusual lability of the chelating diphosphine. This is demonstrated by its reactions with $Ph_2P(CH_2)_nPPh_2$ (n = 1 or 2) both of which give $[Rh(L–L)_2]^+$. More surprisingly, considering its lability in $[Rh(nbd)(dppf)]^+$, dppf also readily displaced disoppf from **4**, to give $[Rh(nbd)(dppf)][BF_4]$ **5**. The nbd ligand in this complex is not displaced by reaction with an excess of dppf.

We have been investigating the activities of iridium catalysts of the types $[Ir(cod)(PR_3)_2]^+$ and $[Ir(cod)(py)(ER_3)]^+$ (cod = cycloocta-1,5-diene, py = pyridine, E = As or P, R = aryl)[1,2] in the homogenous hydrogenation of imines and have found that they are, in general, superior to rhodium analogues.[3] Rhodium complexes incorporating chelating diphosphines with a ferrocene backbone have proved to be useful catalysts for the reduction of carbon–carbon double bonds. For example, $[Rh(nbd)(L–L)]^+$ {nbd = norbornadiene (bicyclo-[2.2.1]hepta-2,5-diene); L–L = 1,1′-bis(diphenylphosphino)-ferrocene (dppf) or 1,1′-bis(di-*tert*-butylphosphino)ferrocene (dbpf)} catalyse the hydrogenation of α,β-unsaturated carboxylic acids.[4] Rhodium–dppf systems have also been successfully employed in the hydroformylation of hex-1-ene,[5] methyl methacrylate[6] and allyl alcohol.[7] Chirality can be readily introduced α to one of the C_5H_4 rings of a ferrocene diphosphine to give compounds with both a conventional chiral centre, and planar chirality, such as those shown in Fig. 1. These all induce moderate to high enantioselectivity in rhodium-catalysed hydrogenation.[8–11] With a view to employing them as imine hydrogenation catalysts, we have studied the synthesis and properties of some Group 9 complexes containing ferrocenyl diphosphine ligands.

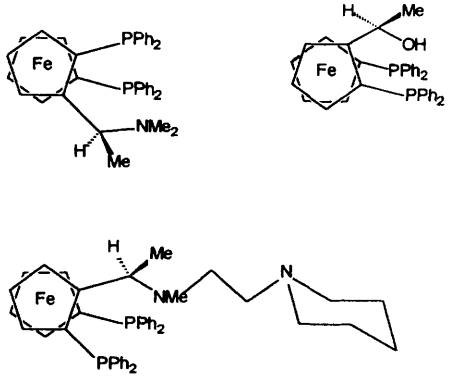

Fig. 1 Chiral ferrocenyl phosphines used in asymmetric hydrogenation

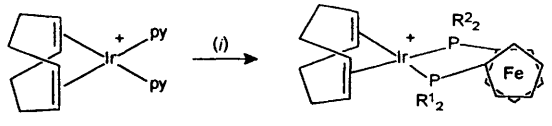

	R^1	R^2
1	Ph	Ph
2	Pr^i	Pr^i
3	Ph	Pr^i

Scheme 1 Synthesis of complexes **1**–**3**: (i) ferrocenyl diphosphine, MeOH

Results and Discussion

1,1′-Bis(diisopropylphosphino)ferrocene (disoppf) and 1-(diisopropylphosphino)-1′-(diphenylphosphino)ferrocene (dipdppf) were prepared by modifications of published procedures.[12] Both of these compounds, as well as dppf, react smoothly with $[Ir(cod)(py)_2][PF_6]$ to form $[Ir(cod)(L–L)][PF_6]$ (L–L = dppf **1**, disoppf **2** or dipdppf **3**) in moderate to good yield (Scheme 1). The deep purple-red complexes display substantial variation in their stability; whilst **1** is stable in moist, aerobic solutions for several weeks, and **2** is indefinitely stable in the solid state, crystals of **3** decompose in air overnight to a tan solid.

The structure of complex **3** (Fig. 2) was determined in an X-ray diffraction study; selected bond lengths and angles are given in Table 1. The final difference map shows a peak of *ca.* 6

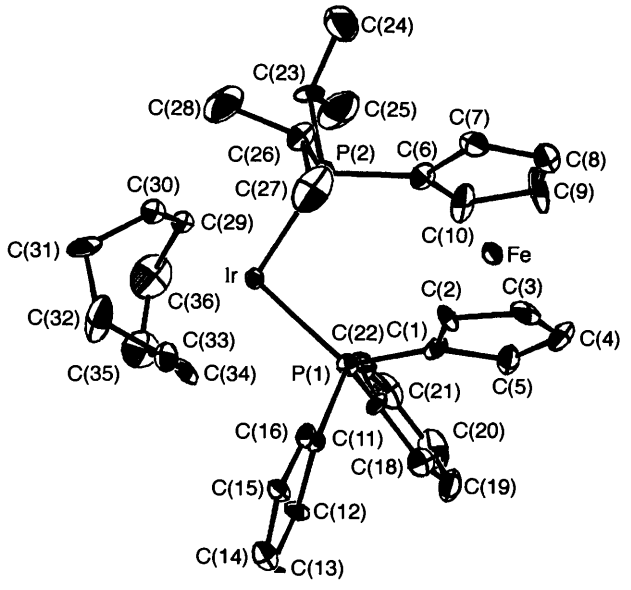

Fig. 2 Molecular structure and numbering scheme of the cation of [Ir(cod)(dipdppf)][PF_6] **3**

Table 1 Selected bond lengths (Å) and angles (°) for complex **3**

Ir–M1	2.115(9)	Ir–M2	2.112(9)
Ir–P(1)	2.358(2)	Ir–P(2)	2.341(2)
Ir–C(29)	2.218(9)	Ir–C(30)	2.233(9)
Ir–C(33)	2.194(9)	Ir–C(34)	2.246(8)
Fe–Cp1	1.625(9)	Fe–Cp2	1.633(9)
P(1)–Ir–P(2)	99.37(7)	M1–Ir–M2	83.7(3)
M1–Ir–P(1)	164.4(2)	M2–Ir–P(2)	167.7(2)
M1–Ir–P(2)	91.0(2)	M2–Ir–P(1)	88.2(2)
Cp1–Fe–Cp2	177.4(4)		

M1 and M2 are the midpoints of the C(29)–C(30) and C(33)–C(34) bonds respectively; Cp1 and Cp2 are the centroids of the C(1)–C(5) and C(6)–C(10) rings.

e $Å^{-3}$ lying on a line joining the Ir and Fe atoms at 2.5 Å from Ir and 1.9 Å from Fe. The data collection had also been undertaken at low temperature (173 K), but the same problem arose on refinement; consequently, we presume this to be an artefact, although we cannot explain its origin.

We have previously reported the single-crystal structures of complex **1**[13] and the tetraphenylborate salt of **2**.[1] A comparison of structural parameters for **1**–**3** is given in Table 2 (see Fig. 3 for definitions). In all three complexes similar bonds to the metal centre have comparable lengths. Likewise there is little difference in either the cod bite angles or those of the diphosphines. Whilst the Cp1–Fe–Cp2 geometry is essentially linear in all cases, the angle of twist about the ferrocene moiety away from the conformation with eclipsed phosphine substituents (angle α in Fig. 3) decreases considerably with increasing steric bulk of the phosphine substituents. Meanwhile, the dihedral angles between the planes defined by P–Ir–P and M–Ir–M (angle β in Fig. 3) markedly increase with the steric profile of the ligands. In all cases the M–Ir–P (*trans*) angle is significantly less than the ideal 180°. There is considerable opening up of the M–Ir–P (*cis*) angle on changing from aryl to alkyl substituents at phosphorus, with concomitant closing of M–Ir–P (*trans*). This is presumably due to unfavourable steric interactions between the substituents at phosphorus and the cod ligand. Therefore, it seems that steric constraint is relieved not by opening up the dipohosphine bite angle, or closing that of the cod ligand, but rather by perturbation of the geometry at iridium away from square planar towards tetrahedral. In order

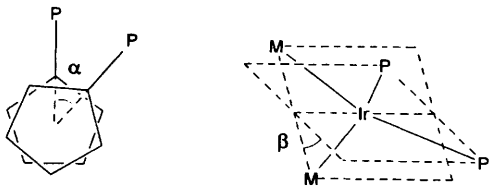

Fig. 3 Definition of α, the angle twist about the ferrocene from eclipsed phosphine substituents, and β, the dihedral angle between planes described by P–Ir–P and M1–Ir–M2 bites

Table 2 A comparison of some structural parameters of complexes **1**–**3**

	1	**2**	**3**
P–Ir/Å	2.352 (mean)	2.336 (mean)	2.349 (mean)
M–Ir/Å	2.096 (mean)	2.085 (mean)	2.113 (mean)
Cp–Fe–Cp/°	178.9	179.2(8)	177.4(4)
P–Ir–P/°	99.2(1)	99.4(1)	99.37(7)
M1–Ir–M2/°	83.4	84.1(7)	83.7(3)
M–Ir–P(*cis*)/°	87.75 (mean)	91.55 (mean)	89.6 (mean)
M–Ir–P(*trans*)/°	171.8 (mean)	159.0 (mean)	166.0 (mean)
α*/°	41.4 ± 0.80	25.8 ± 2.58	33.22 ± 0.69
β*/°	3.2	27.5	16.2

* See Fig. 3 for definition of α and β.

to maintain the ideal bite angle the ferrocene moiety is forced to adopt a conformation closer to that with the phosphine-bearing carbons eclipsed, as the bulk of the phosphorus substituents increases.

All three molecules have a chiral centre at iridium in the solid state as a consequence of the twist about the ferrocene moiety. Variable-temperature NMR spectroscopic studies were performed on **2** to see if stereochemical non-rigidity is observed in the solution state. Fig. 4 shows the ^1H NMR spectrum recorded at 298 and 186 K. At low temperature two distinct magnetic environments are observed for the cod alkene protons with signals at δ 5.19 and 3.80. Examination of the solid-state structure of the complex, which we assume to be close to the low-temperature static structure observed by NMR spectroscopy, shows clearly that the two ends of each carbon–carbon double bond are different. One CH of each bond is directed towards an isopropyl group, and the other towards a relatively empty region of space. This is reflected in the 1.4 ppm separation of the =CH peaks. It is not possible to be certain which resonance should be assigned to which =CH peak. We hoped to observe a nuclear Overhauser effect (NOE) between one type of =CH and the isopropyl groups but the low-temperature NOE experiment gave equivocal results. Four environments are obvious for the cyclopentadienyl protons with signals at δ 4.51, 4.38, 4.34 and 4.31, as well as four distinct methyl environments with resonances at δ 1.73, 1.38, 1.04 and 0.64. This is indicative of a slow interchange of the stereoisomeric conformers shown in Scheme 2, with the low-temperature spectrum reflecting the limiting enantiomeric structures. Similar results have been observed for the platinum complex [PtR_2(dppf)] (R = CH_2-$SiMe_2CH{=}CH_2$).[14] It is also notable that a single sharp ^{31}P resonance is observed for each of the complexes throughout the accessible temperature range. This may indicate that the phosphorus centres remain rigorously identical despite the breaking of symmetry in other parts of the molecule. However, it is also possible that the phosphorus atoms become magnetically distinct at low temperature, but their chemical shifts are still too similar for resolution.

At higher temperatures rapid exchange of conformations gives rise to a time-averaged spectrum, the full assignment of which is given in the Experimental section. Fig. 5 shows the

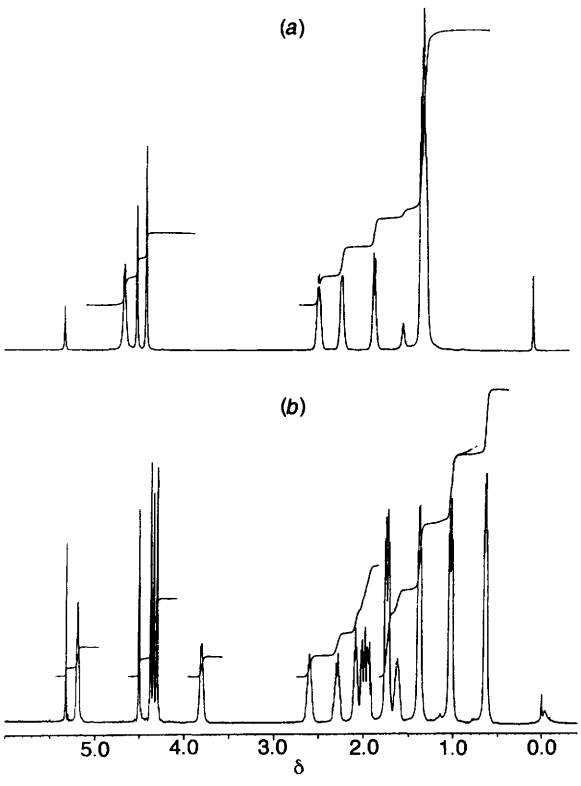

Fig. 4 The 500 MHz ^{1}H NMR spectra of complex **2** recorded at (*a*) 298 and (*b*) 186 K

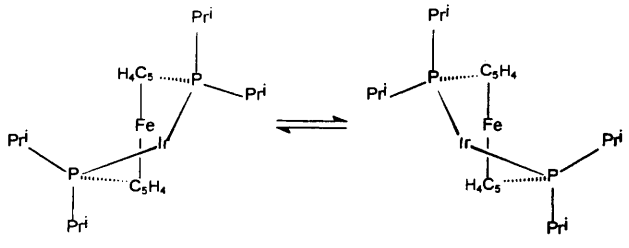

Scheme 2 Interchange of stereoisomeric conformers of complex **2**

cyclopentadienyl region of the spectrum recorded at various temperatures. Two coalescences are obvious, with the inner two peaks coalescing at 206 ± 1 K and the outer two between 207 and 239 K. By inserting the former value into the Eyring equation,[15] $\Delta G^{\ddagger} = RT_c[22.96 + (\ln T_c/\Delta\nu)]$, an approximate value for the barrier to interconversion of the conformers of 39.3 ± 0.2 kJ mol^{-1} is obtained ($\Delta\nu$ = 16.2 Hz). Similar experiments on **1** and **3** showed that these molecules undergo analogous processes, with $\Delta G^{\ddagger}$ values of 36.1 ± 0.2 and 34.3 ± 0.2 kJ mol^{-1} respectively.

The homoleptic species $[M(dppf)_2]^+$ (M = Rh or Ir) have been reported[16] and, in the case of M = Ir, the single-crystal structure has been determined. It was found that the geometry at the iridium atom was severely distorted from square planar towards tetrahedral with a dihedral angle between the planes described by the two P–Ir–P bite angles of 51°. We were therefore interested to synthesize the species $[M(disoppf)_2]^+$ or $[M(disoppf)(dppf)]^+$ (M = Rh or Ir), as it would be expected that the geometry about the M atom would be distorted even further towards tetrahedral in these cases. So far we have been unsuccessful, but one of the complexes prepared, [Rh(nbd)(disoppf)][BF$_4$] **4**, has shown some intriguing ligand-substitution chemistry.

It is well known that the reaction of 2 equivalents of dppe with $[Rh(nbd)_2]^+$ leads to the formation of $[Rh(dppe)_2]^+$[17] (Scheme 3); we therefore hoped that a similar methodology

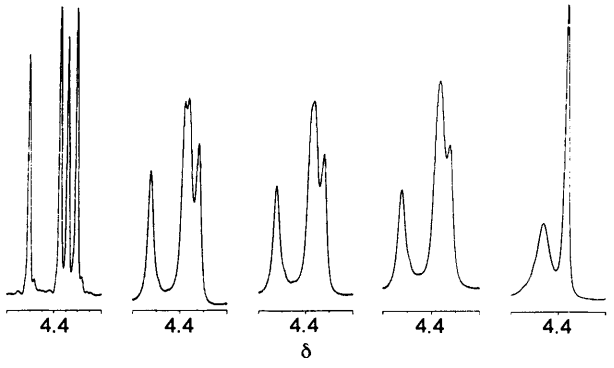

Fig. 5 Cyclopentadiene region of the 500 MHz spectrum of complex **2** recorded at (from left to right) 186, 205, 206, 207 and 239 K

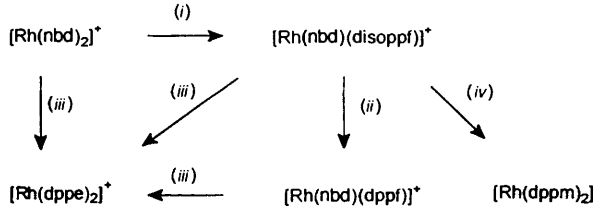

Scheme 3 Ligand-substitution reactions: (*i*) disoppf, CH_2Cl_2; (*ii*) dppf, $CDCl_3$; (*iii*) dppe ($Ph_2PCH_2CH_2PPh_2$), $CDCl_3$; (*iv*) dppm ($Ph_2PCH_2PPh_2$), $CDCl_3$

could be applied to the synthesis of $[Rh(disoppf)_2]^+$. However, addition of 2 equivalents of disoppf to $[Rh(nbd)_2][BF_4]$ in dichloromethane led exclusively to the formation of [Rh(nbd)(disoppf)][BF$_4$] **4**. The reactions of **4** with less bulky chelating diphosphines were attempted in order to determine whether they would give complexes of the type [Rh(disoppf)(L–L)][BF$_4$] (L–L = diphosphine), which would still be expected to show severe distortion from square-planar geometry. Complex **4** was treated with a ten-fold excess of dppf in $CDCl_3$ solution in a 5 mm NMR tube. The ^{31}P-{^{1}H} NMR spectrum recorded after 1 h showed the presence of free dppf, disoppf and the known complex[4] [Rh(nbd)(dppf)][BF$_4$] **5**, only. Whilst the preferential replacement of a chelating dipohosphine over an alkene by a second diphosphine has been noted for complexes of Pd^0[18] and Pt^0,[19] to the best of our knowledge this type of substitution reaction at a Group 9 metal is unprecedented. Evidently **5** shows no tendency to undergo replacement of nbd with a second dppf ligand to form the bis(dppf) species.

The reactivity of complex **4** towards dppe was also examined on an NMR-tube scale. The ^{31}P-{^{1}H} NMR spectrum of a reaction mixture of **4** with a ten-fold excess of dppe in $CDCl_3$ recorded after 15 min showed the presence of [Rh(dppe)$_2$][BF$_4$] **6** as the sole rhodium-containing species. When the amount of dppe was restricted to 1 equivalent and the reaction was repeated, only peaks corresponding to **4** and **6** were observed in the ^{31}P-{^{1}H} NMR spectrum. From these data it is not possible to determine whether the disoppf ligand is substituted by dppe prior to the nbd ligand. However, whichever intermediate is formed, it is more reactive with dppe than is **4**. The positive-ion FAB mass spectrum of the residue from a reaction of **4** with dppe halted after 1 min by rapid removal of the dichloromethane solvent threw no light on the nature of the intermediate, being a composite of those recorded for **4** and **6**. The NMR-tube-scale reaction of **4** with 1.5 equivalents of dppm showed, after 15 min, the presence of **4** and the previously reported $[Rh(dppm)_2]^+$,[20] indicative of an analogous ligand-exchange reaction.

In order to establish whether any unusual structural characteristics cause increased lability of the diphosphine ligand, the

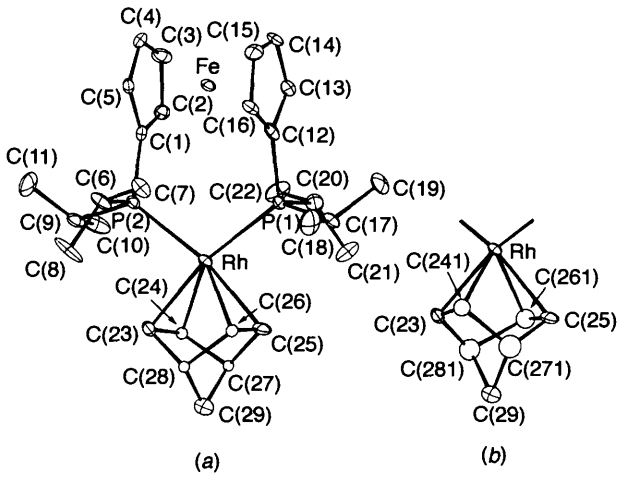

Fig. 6 Molecular structure and numbering schemes of the two conformers of the cation of [Rh(nbd)(disoppf)][BF_4] **4**

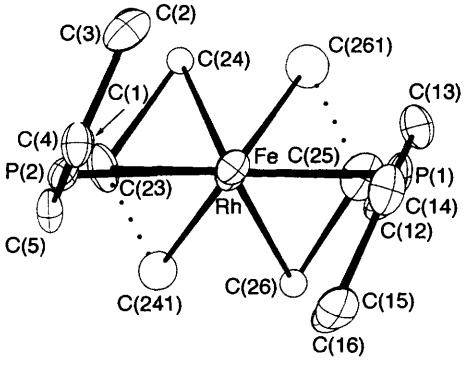

Fig. 7 View along the Fe···Rh axis of complex **4**

Table 3 Selected bond lengths (Å) and angles (°) for complex **4**

Rh–M1	2.24	Rh–M2	2.13
Rh–M3	2.01	Rh–M4	2.12
Rh–P(1)	2.354(3)	Rh–P(2)	2.352(3)
Rh–C(23)	2.20(1)	Rh–C(24)	2.24(2)
Rh–C(25)	2.22(1)	Rh–C(26)	2.25(2)
Rh–C(241)	2.01(3)	Rh–C(261)	2.23(3)
Fe–Cp1	1.64	Fe–Cp2	1.64
P(1)–Ir–P(2)	100.91(10)	Cp1–Fe–Cp2	178.0
M1–Rh–M2	68.3	M3–Rh–M4	72.8
M1–Rh–P(1)	135.3	M3–Rh–P(1)	157.5
M2–Rh–P(1)	97.7	M4–Rh–P(1)	96.3
M1–Rh–P(2)	108.8	M3–Rh–P(2)	95.2
M2–Rh–P(2)	154.0	M4–Rh–P(2)	157.6

Cp1 and Cp2 are the centroids of the C(1)–C(5) and C(12)–C(16) rings; M1, M2, M3 and M4 are the midpoints of the C(23)–C(24), C(25)–C(26), C(23)–C(241)and C(25)–C(261) bonds respectively.

single-crystal structure of complex **4** was determined. The nbd ligand is disordered between two orientations sharing the common C(23), C(25) and C(29) positions. The structure of one molecule is shown in Fig. 6(*a*), with the inset 6(*b*) showing the alternative sites. Selected bond lengths and angles are given in Table 3. Fig. 7 shows the view along the Fe···Rh axis. The conformation shown in Fig. 6(*a*) is grossly similar to that in **2**, with alkene and C_5H_4 moieties adopting a *syn* disposition, whilst in the conformer shown in Fig. 6(*b*) they adopt an *anti* conformation.

The P–M–P bite angle in complex **4** is slightly larger than that in **2**, and smaller than that in the analogous [Rh(nbd)(dbpf)]$^+$ [103.71(5)°].[4] The average P–M bond length (2.353 Å) is shorter than that in **2**, reflecting the lower covalent radius of rhodium. The twist about the ferrocenyl moiety, α, is 27.20(9)°, about the same as that in **2**. The two conformations of **4** have remarkably different dihedral angles between the planes defined by the bites of the disoppf and nbd ligands, β, of 49.26(7)° for the *syn* and 25.83(11)° for the *anti* conformation. The former angle is considerably greater than the analogous one in **2**, and is also greater than the equivalent angle in [Rh(nbd)(dbpf)]$^+$ (36.8°).[4] This larger distortion around the metal centre, caused presumably by the smaller covalent radius of rhodium, may account for the lability of the diphosphine and the unwillingness of rhodium to accommodate two disoppf ligands.

Further investigations are necessary to determine the mechanism and scope of these unusual substitution reactions. We are also currently examining the reactions of [$Rh(MeOH)_2$(dppf)]$^+$, obtained on hydrogenation of **5**, with chelating and monodentate phosphines, including disoppf, and exploring the potential of these complexes in the catalytic hydrogenation of imines.

Experimental

The complexes [Ir(cod)(dppf)][PF_6] **1**,[13] [Ir(cod)$(py)_2$][PF_6][21] and [$Rh(nbd)_2$][BF_4][22] were prepared according to literature methods.

Reaction procedures

All reactions were performed under an atmosphere of dry nitrogen using standard Schlenk techniques. Solvents were freshly distilled under nitrogen prior to use, ethers from sodium–potassium alloy, dichloromethane from calcium hydride and alcohols from their magnesium alkoxides. Elemental analyses were performed by Medac Ltd., Brunel University. The NMR spectra were recorded on Bruker AMX500 or AC250Y spectrometers, with ^{1}H shifts referenced to internal solvent, and reported in ppm downfield from $SiMe_4$; ^{31}P chemical shifts are reported in ppm downfield from external 85% H_3PO_4. The FAB mass spectra were recorded on a Kratos 80RF spectrometer coupled to a Kratos DS55M data system using 3-nitrobenzyl alcohol as a solvent.

Preparations

[Ir(cod)(disoppf)][PF_6] 2. A mixture of [Ir(cod)$(py)_2$][PF_6] (1.096 g, 1.82 mmol) and 1,1′-bis(diisopropylphosphino)-ferrocene (0.80 g, 1.90 mmol) in methanol (40 cm^3) was stirred overnight, during which time a red-brown precipitate formed. The supernatant was removed with a syringe and retained. The residue was washed with methanol (2 × 10 cm^3), leaving a small amount of pure product. The combined washings and supernatant liquid were concentrated *in vacuo* and cooled, yielding a second crop of product. The solvent was removed from this second crop which was recrystallised (dichloromethane–diethyl ether) to give complex **2** as a red-purple solid (0.60 g, 37%, not optimised) (Found: C, 41.3; H, 5.4; $C_{30}H_{48}F_6FeIrP_3$ requires C, 41.7; H, 5.6). δ_H(500 MHz, CD_2Cl_2) 1.53 [12 H, m, $PCH(CH_3)_2$], 1.85 (4 H, m, cod CH_2), 2.21 (4 H, s, br, cod CH_2), 2.48 [4 H, m, $PCH(CH_3)_2$], 4.41 (4 H, s, C_5H_4), 4.52 (4 H, s, C_5H_4) and 4.66 (4 H, s, cod C=CH). δ_P(100 MHz, $CDCl_3$) 27.66 (s, PPr^i_2) and −142.83 [spt, *J*(PF) 712.5 Hz, PF_6]. Positive-ion FAB mass spectrum: *m/z* 719 (M^+) and 611 (M^+ − cod).

[Ir(cod)(disoppf)][BPh_4]. A solution of sodium tetraphenylborate (1.0 g, 2.9 mmol) in water (15 cm^3) was added to a solution of [Ir(cod)(disoppf)][PF_6] (0.123 g, 0.14 mmol) in dichloromethane (5 cm^3) and the resultant two-phase system was stirred vigorously for 20 min. The aqueous phase was removed with a syringe and the dichloromethane layer washed with water (3 × 5 cm^3). The solvent was removed *in vacuo* and the residue recrystallised (dichloromethane–diethyl ether) to give [Ir(cod)(disoppf)][BPh_4] as deep purple blocks (0.12 g, 94%).

Table 4 Conditions for 5 mm NMR-tube-scale reactions

Reaction	4 + dppf	4 + dppe	4 + dppe	4 + dppm	6 + dppe
Amount of complex/mg (μmol)	8.0 (11.4)	5.9 (8.4)	6.1 (8.7)	13.8 (19.7)	15.2 (18.2)
Amount of diphosphine/mg (μmol)	67.0 (120.9)	3.6 (9.0)	35.2 (88.3)	11.0 (28.6)	7.5 (18.8)
Reaction time/min	60	20	10	15	20

δ_H(250 MHz, $CDCl_3$) 1.32 [24 H, m, $PCH(CH_3)_2$], 1.85 (4 H, m, cod CH_2), 2.23 (4 H, m, cod CH_2), 2.47 [4 H, m, $PCH(CH_3)_2$], 4.42 (4 H, m, C_5H_4), 4.52 (4 H, m, C_5H_4), 4.65 (4 H, s, br, cod C=CH) and 6.9–7.5 [20 H, m, $B(C_6H_5)_4$]. $\delta_P(CDCl_3)$ 27.67 (s, PPr^i_2).

[Ir(cod)(dipdppf)][PF_6] 3. A mixture of [Ir(cod)(py)$_2$][PF_6] (0.168 g, 0.279 mmol) and dipdppf (0.124 g, 0.255 mmol) in methanol (20 cm^3) was stirred for 7 h. The resulting suspension was cooled to −20 °C overnight, then the supernatant was removed by syringe. The residue was washed (diethyl ether) and recrystallised (dichloromethane–diethyl ether) yielding complex **3** as maroon blocks (0.17 g, 72%) (Found: C, 46.25; H, 4.7. $C_{36}H_{44}F_6FeIrP_3$ requires C, 46.4; H, 4.8%). $\delta_H(CDCl_3)$ 1.40 [12 H, m, $PCH(CH_3)_2$], 1.73 (2 H, m, cod CH_2), 2.03 (4 H, m, cod CH_2), 2.32 (2 H, m, cod CH_2), 2.59 [2 H, m, $PCH(CH_3)_2$], 3.85 (2 H, s, cod C=CH), 4.26 (2 H, s, C_5H_4), 4.38 (4 H, s, C_5H_4), 4.52 (2 H, s, C_5H_4), 4.96 (2 H, s, cod C=CH), 7.54 (6 H, m, Ph) and 7.81 (4 H, m, Ph). $\delta_P(CDCl_3)$ 25.33 [d, J(PP) 16.0, PPr^i_2] and 14.86 [d, J(PP) 16.5 Hz, PPh_2]. Positive-ion FAB spectrum: *m/z* 787 (M^+), 705 and 633.

Reaction of [Rh(nbd)$_2$][BF_4] with 2 equivalents of disoppf. A solution of [Rh(nbd)$_2$][BF_4] (0.015 g, 0.041 mmol) and disoppf (0.034 g, 0.081 mmol) in dichloromethane (2 cm^3) was stirred for 15 min, then concentrated *in vacuo* to about 0.5 cm^3 and diethyl ether (20 cm^3) added. Removal of the supernatant *via* cannula and recrystallisation (dichloromethane–diethyl ether) gave orange crystals of [Rh(nbd)(disoppf)][BF_4] **4** (0.021 g, 74%) (Found: C, 49.2; H, 6.2. $C_{29}H_{44}BF_4FeP_2Rh$ requires C, 49.7; H, 6.3%). $\delta_H(CDCl_3)$ 1.21 [12 H, d of d, J(HH) 6.8, J(PH) 14.1, $PCHCH_3$], 1.49 [12 H, d of d, J(HH) 7.3 Hz, J(PH) 15.7, $PCHCH_3'$], 1.78 (2 H, s, nbd CH_2), 2.35 [4 H, m, $PCH(CH_3)_2$], 4.18 (2 H, s, br, nbd CH_2CH), 4.37 (4 H, s, br, C_5H_4), 4.48 (4 H, m, C_5H_4') and 5.17 [4 H, d of d, J(HH) 2.0, J(RhH) 4.8 Hz, nbd C=CH]. $\delta_P(CDCl_3)$ 39.60 [d, J(RhP) 158.6 Hz]. Positive-ion FAB mass spectrum: *m/z* 613 (M^+), 525 ($M^+ - 2H - 2Pr^i$) and 439 ($M^+ - 2H - 4Pr^i$).

NMR-scale reactions

A solution of the appropriate complex and diphosphine (see Table 4 for conditions) in $CDCl_3$ (0.4 cm^3) in a 5 mm NMR tube was allowed to stand at room temperature. The ^1H (250 MHz) and ^{31}P-{^1H} (100 MHz) NMR spectra were recorded at various intervals.

Crystallography

Single crystals of complexes **3** and **4** were grown from dichloromethane layered with diethyl ether; the dimensions of the crystals used in the determinations were 0.2 × 0.1 × 0.15 and 0.4 × 0.2 × 0.1 mm respectively. Diffraction data were collected with graphite-monochromated Mo-Kα radiation (λ = 0.7107 Å) on an Enraf-Nonius CAD-4 diffractometer at 293 and 173 K for **3** and **4** respectively.

Complex 3. *Data collection and processing.* θ–2θ mode, $2 < \theta < 30°$, h 0–18, k 0–20, l −26 to 26. 11068 Reflections measured, 10681 unique, 6883 significant, $|F^2| > 2\sigma(F^2)$, R_{int} 0.03. Maximum change in standard reflections −2.5%, no decay correction. Absorption correction t_{max} 1.000, t_{min} 0.68 from ψ-scan data.

Table 5 Crystallographic data for compounds **3** and **4**

	3	**4**·Et_2O
Formula	$C_{36}H_{44}F_6FeIrP_3$	$C_{33}H_{54}BF_4FeOP_2Rh$
M	931.7	774.3
Crystal system	Monoclinic	Monoclinic
Space group	$P2_1/n$ (non-standard no. 14)	$P2_1/c$ (no. 14)
a/Å	13.405(2)	15.277(4)
b/Å	14.540(2)	10.173(7)
c/Å	18.740(5)	20.529(8)
β/°	104.14(2)	94.54(3)
U/Å^3	3541.8	3181(3)
D_c/g cm^{-3}	1.75	1.62
Z	4	4
μ/cm^{-1}	43.4	11.3
$R1$	0.059	0.099
R'	0.059	—
$wR2$ (all data)	—	0.310
$F(000)$	1848	1608
Goodness of fit, S	1.5	1.05

$R1 = \Sigma(|F_o| - |F_c|)/\Sigma|F_o|$, $R' = [\Sigma w(|F_o| - |F_c|^2/\Sigma w|F_o|^2]^{\frac{1}{2}}$, $wR2 = [\Sigma w(|F_o|^2 - |F_c|)^2/\Sigma w|F_o|^4]^{\frac{1}{2}}$ and $w = \sigma^{-2}(F)$ with $\Sigma w(|F_o| - |F_c|)^2$ minimised.

Structure analysis and refinement. Heavy-atom methods, SHELXS 86,[23] refinement by full-matrix least squares. Non-H atoms anisotropic, Enraf-Nonius MOLEN programs.[24] Hydrogen atoms fixed at calculated positions, $U_{iso} = 1.3U_{eq}$ for parent atom, 424 variables, $(\Delta\sigma)_{max}$ 0.01, $(\Delta\rho)_{max,min}$ +5.97, −0.44 e Å^{-3}. A previous structure determination of this complex at low temperature showed a large residual peak in the final difference map between the Ir and Fe atoms. Since this might have been the result of some problems of icing up of the crystal during data collection it was decided to repeat the determination. The results given are from this second data collection at room temperature using a different crystal from the same batch. However, the final difference map again showed a peak of *ca.* 6 e Å^{-3} lying on a line joining the Ir and Fe atoms at 2.5 Å from Ir and 1.9 Å from Fe. We presume that this is an artefact, but cannot explain its origin.

Complex 4. *Data collection and processing.* θ–2θ mode, $2 < \theta < 25°$, h 0–18, k 0–12, l −24 to 24. 5792 Reflections measured, 5579 unique, 4026 significant, $|F^2| > 2\sigma(F^2)$, R_{int} 0.042. Maximum change in standard reflections −2%, no decay correction. Absorption correction t_{max} 1.00, t_{min} 0.91 from ψ-scan data.

Structure analysis and refinement. Direct methods, SHELXS 86, refinement by full-matrix least squares on F^2 using SHELXL 93.[25] Non-H atoms anisotropic. The nbd ligand is disordered between two orientations sharing common C(23), C(25) and C(29) positions. The half-occupancy sites were refined with isotropic thermal parameters. Other non-H atoms were anisotropic. Hydrogen atoms were included in the riding mode with $U_{iso} = 1.2U_{eq}$(C) or $1.5U_{eq}$(C) for methyl groups, but were omitted for the disordered nbd ligand. Unresolved electron density near 0, 0, ½ was assumed to be disordered ether solvate and was modelled as five anisotropic C atoms without H atoms [C(30)–C(34)]. 384 Variables $(\Delta\sigma)_{max}$ 0.001, $(\Delta\rho)_{max,min}$ +2.13, −4.72 e Å^{-3}.

Crystallographic data for both complexes are given in Table 5.

Atomic coordinates, thermal parameters, and bond lengths and angles have been deposited at the Cambridge Crystallographic Data Centre (CCDC). See Instructions for Authors,

J. Chem. Soc., Dalton Trans., 1996, Issue 1. Any request to the CCDC for this material should quote the full literature citation and the reference number 186/265.

Acknowledgements

We thank the University of Sussex for the provision of a bursary (to R. B. B.) and Johnson-Matthey for a generous loan of rhodium and iridium salts.

References

1 R. B. Bedford, P. A. Chaloner, C. Claver, E. Fernandez, P. B. Hitchcock and A. Ruiz, in *Catalysis of Organic Reactions (Chemical Industries Series 62)*, eds. M. G. Scaros and M. L. Prunier, Marcel Dekker, 1994, pp. 181–188.
2 R. B. Bedford, P. A. Chaloner, S. Z. Dewa, G. López, P. B. Hitchcock, F. Momblona and J. L. Serrano, *J. Organomet. Chem.*, in the press.
3 C. J. Longley, T. J. Goodwin and G. Wilkinson, *Polyhedron*, 1986, **5**, 1625.
4 W. R. Cullen, T. J. Kim, F. W. B. Einstein and T. Jones, *Organometallics*, 1983, **2**, 714.
5 P. Kalck, C. Randrianalimanan, M. Ridmy and A. Thorez, *New J. Chem.*, 1988, **12**, 679.
6 C. U. Pittman, W. D. Honnick and J. J. Yang, *J. Org. Chem.*, 1980, **45**, 684.
7 C. U. Pittman and W. D. Honnick, *J. Org. Chem.*, 1980, **45**, 2132.
8 T. Hayashi and M. Kumada, *Acc. Chem. Res.*, 1982, **15**, 395.
9 T. D. Appleton, W. R. Cullen, S. V. Evans, T.-J. Kim and J. Trotter, *J. Organomet. Chem.*, 1985, **279**, 5.
10 T. Hayashi, N. Kawamura and Y. Ito, *J. Am. Chem. Soc.*, 1987, **109**, 7876.
11 T. Hayashi, N. Kawamura and Y. Ito, *Tetrahedron Lett.*, 1988, **29**, 5969.
12 I. R. Butler, W. R. Cullen and T.-J. Kim, *Synth. React. Inorg. Metal-Org. Chem.*, 1985, **15**, 109.
13 R. B. Bedford, P. A. Chaloner and P. B. Hitchcock, *Acta Crystallogr., Sect. C*, 1993, **49**, 1614.
14 R. B. Kelly and G. B. Young, *Polyhedron*, 1989, **8**, 433.
15 H. Shanan-Atidi and K. H. Bar-Eli, *J. Phys. Chem.*, 1970, **74**, 961.
16 U. Casellato, B. Corain, R. Graziani, B. Longato and G. Pilloni, *Inorg. Chem.*, 1990, **29**, 1193.
17 P. A. Chaloner, unpublished work.
18 G. T. L. Broadwood-Strong, P. A. Chaloner and P. B. Hitchcock, *Polyhedron*, 1993, **12**, 721.
19 P. A. Chaloner and G. T. L. Broadwood-Strong, *J. Organomet. Chem.*, 1989, **362**, C21.
20 L. H. Pignolet, D. H. Doughty, S. C. Nowicki and A. L. Casalnuovo, *Inorg. Chem.*, 1980, **19**, 2172.
21 R. H. Crabtree and S. M. Morehouse, *Inorg. Synth.*, 1974, **15**, 19.
22 R. Uson, L. A. Oro, M. A. Garralda, C. Claver and P. Laheurta, *Transition Met. Chem.*, 1979, **4**, 55.
23 G. M. Sheldrick, SHELXS 86, University of Göttingen, 1986.
24 MOLEN, CAD4 software version 5.0, Enraf-Nonius, Delft, 1989.
25 G. M. Sheldrick, SHELXL 93, University of Göttingen, 1993.

Received 25*th July* 1996; *Paper* 6/05192H